AGU PUBLICATIONS

Geophysical Research Letters

RESEARCH LETTER
10.1002/2017GL076015

Key Points:
- Using repeated temperature-depth profiles, the rate of migration of the inflection point can be used as a tracer for groundwater flow
- A numerical model of coupled heat flow and groundwater flow is in excellent agreement with observed trends
- Monitoring the inflection point position could potentially be used to inform sustainable groundwater resources management

Correspondence to:
V. F. Bense,
victor.bense@wur.nl

Citation:
Bense, V. F., & Kurylyk, B. L. (2017). Tracking the subsurface signal of decadal climate warming to quantify vertical groundwater flow rates. *Geophysical Research Letters*, *44*, 12,244–12,253. https://doi.org/10.1002/2017GL076015

Received 14 JUN 2017
Accepted 28 NOV 2017
Accepted article online 4 DEC 2017
Published online 29 DEC 2017

Tracking the Subsurface Signal of Decadal Climate Warming to Quantify Vertical Groundwater Flow Rates

V. F. Bense[1] **and B. L. Kurylyk**[2]

[1]Department of Environmental Sciences, Wageningen University, Wageningen, Netherlands, [2]Department of Civil and Resource Engineering, Dalhousie University, Halifax, Nova Scotia, Canada

Abstract Sustained ground surface warming on a decadal time scale leads to an inversion of thermal gradients in the upper tens of meters. The magnitude and direction of vertical groundwater flow should influence the propagation of this warming signal, but direct field observations of this phenomenon are rare. Comparison of temperature-depth profiles in boreholes in the Veluwe area, Netherlands, collected in 1978–1982 and 2016 provided such direct measurement. We used these repeated profiles to track the downward propagation rate of the depth at which the thermal gradient is zero. Numerical modeling of the migration of this thermal gradient "inflection point" yielded estimates of downward groundwater flow rates (0–0.24 m a^{-1}) that generally concurred with known hydrogeological conditions in the area. We conclude that analysis of inflection point depths in temperature-depth profiles impacted by surface warming provides a largely untapped opportunity to inform sustainable groundwater management plans that rely on accurate estimates of long-term vertical groundwater fluxes.

1. Introduction

Subsurface temperature-depth (TD) measurements at a single point in time have been used to infer vertical groundwater flow rates by estimating advective components of heat flow in the conduction dominated thermal regime of the Earth's shallow crust (i.e., <1,000 m) (Saar, 2011). Such estimates have often been obtained using steady state thermal approaches with the inferred groundwater fluxes interpreted to be representative of long-term averages of groundwater recharge or discharge (Bredehoeft & Papadopulos, 1965; Kurylyk et al., 2017; Reiter, 2001). Knowledge of time-averaged vertical groundwater flux rates is essential for sustainable groundwater management to prevent groundwater depletion in the context of climate change, land cover change, and increased demand from global population rise (e.g., Scanlon et al., 2006; Wada et al., 2010). However, it has long been recognized (Ferguson & Woodbury, 2006; Taniguchi et al., 1999) that the ongoing disturbance of the subsurface thermal regime as a result of climate warming and/or land use change (Bense & Beltrami, 2007; Bayer et al., 2016; Menberg et al., 2014) will increasingly hamper such long-term groundwater flux estimates due to a mixing of the thermal disturbances caused by surface warming and groundwater flow (Irvine et al., 2017; Kurylyk & Irvine, 2016).

Sustained surface warming is eventually manifested in the subsurface at depths below the seasonal zone (e.g., 15 m), producing an inversion of the thermal gradient. This deviates from an equilibrium situation in which temperatures generally increase with depth due to upward geothermal heat flow. Hence, in this reverse setting, a depth exists at which the thermal gradient is zero. In this study, we refer to this as the "inflection point depth." Taniguchi et al. (1999) used analytical solutions to a transient equation of fluid and heat flow to show that the rate at which the inflection point depth increases over time is strongly influenced by vertical groundwater flow. They illustrated their approach by comparing observed inflection point depths to analytical solution results for scenarios of ground surface warming, geothermal heat flow, and vertical groundwater flow. However, fundamental shortcomings of the analytical solutions employed by Taniguchi et al. (1999) have recently been discussed in detail elsewhere (Bense et al., 2017). Moreover, for this approach to be evaluated more robustly, repeated TD logging over relatively long periods (e.g., decades) are required to trace the depth propagation of the inflection point in time. Such data were not available to Taniguchi et al. (1999). Repeated thermal profile measurements have been carried out in a few sites, but these studies were conducted in areas with very little groundwater flow and focused on climatological processes

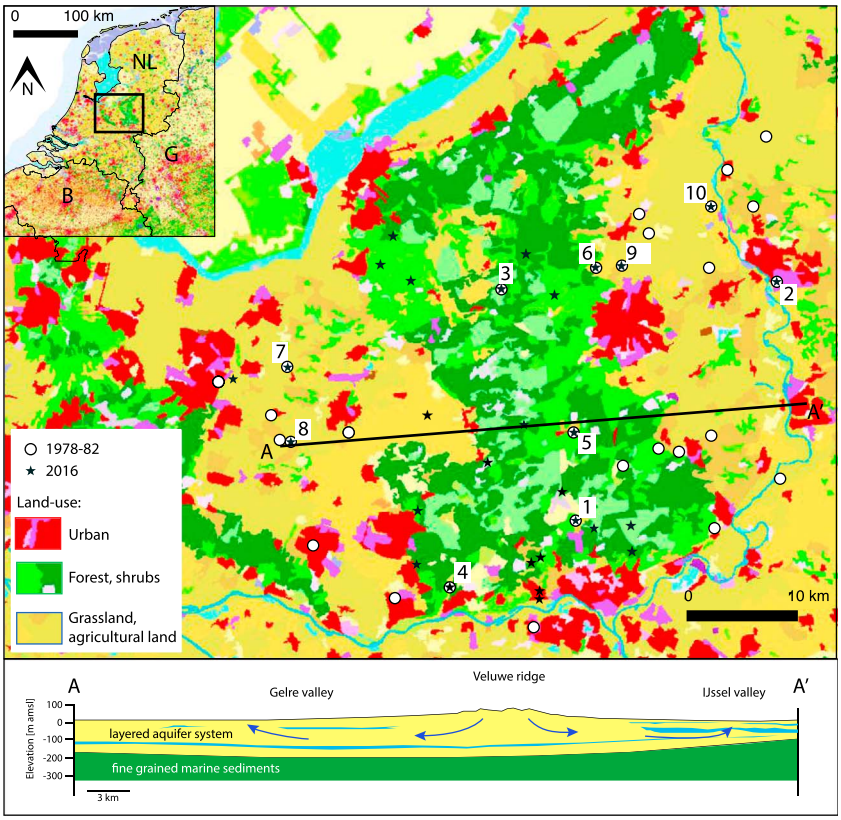

Figure 1. Map of the Veluwe area showing land use and sites of boreholes used in this study. Location of the area is indicated on the inset map of the Netherlands inside the square (NL = Netherlands; G = Germany; B = Belgium). Land use information is from the European Environment Agency data portal and represents the 2012 situation (http://eea.europa.eu). The bottom panel shows a hydrogeological cross section (A-A′) based upon the hydrogeological model of the Netherlands that is maintained by the Dutch Geological Survey (http://dinoloket.nl). The hydrogeological base, through which groundwater flow is assumed negligible, is formed by fine-grained marine sediments (green) that are overlain by a sequence of sandy (yellow) and clayey/silt (bright blue) sediments. General groundwater flow directions are indicated by arrows (dark blue).

(Davis et al., 2010; Dědeček et al., 2012; Harris & Chapman, 2007) or the effects of urbanization (Ferguson & Woodbury, 2007) or land use (Kooi, 2008; MacDougall & Beltrami, 2017) on subsurface temperatures.

Here, we interpret a newly collected data set of TD profiles from the Veluwe area, Netherlands, where TD data were previously recorded in 1978–1982. This unique combined data set illustrates the complex interplay of land use, climate warming, urbanisation, and groundwater flow on subsurface thermal regimes. However, we focus here on the analysis of the inflection point propagation at 10 sites with repeated measurements. In contrast to Taniguchi et al. (1999), we use a numerical one-dimensional heat and groundwater flow model to show that analysis of the inflection point propagation enables the quantitative development of plausible vertical groundwater flow rate estimates. We show that these corroborate with an independent assessment of the hydrogeological regime at each of the 10 borehole sites based on observed vertical hydraulic head gradients at each site. We conclude that subsurface warming signals can be tracked to reliably estimate long-term vertical groundwater flow rates. This technique provides a relatively cheap and straightforward means to evaluate groundwater flow conditions that has to date been largely unexplored.

2. Study Area and Data Collection

Our study area is situated in the Netherlands (Figure 1a) and comprises the topographically elevated Veluwe zone roughly oriented in a north-south direction as well as flanking lower lying valleys of the Grift and IJssel rivers in the east and west, respectively. The upper several hundreds of meters of the study area subsurface is formed by stacks of unconsolidated siliciclastic sediments dating from the Holocene and Pleistocene (Figure 1). These overlay marine fine-grained clayey sediments that are of Miocene age. Push moraines, which

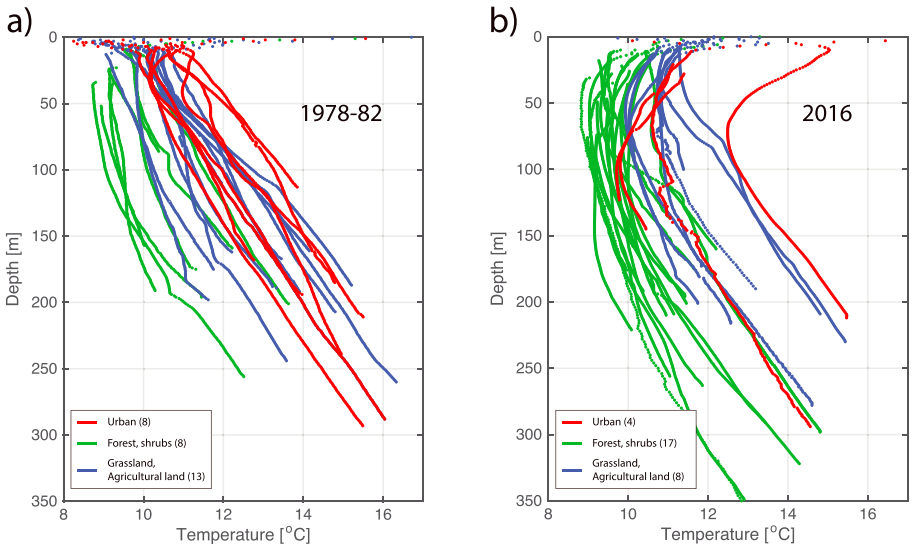

Figure 2. Temperature-depth profiles obtained in (a) 1978–1982 and (b) 2016. For location of sites of observation see Figure 1. Line colors indicate land use at the site of each borehole as indicated in Figure 1. A subset (10) of the TD profiles recorded in 1978–1982 and 2016 were obtained in the same boreholes. These are shown in Figure 3.

formed at the terminus of an ice sheet during the penultimate glacial maximum, are responsible for the current relief in the Veluwe area.

Meteorological records (knmi.nl) representative for the Veluwe area show that annual average air temperature is currently (1996–2016) on average +10.5°C, with a seasonal amplitude of about 8°C. The topographic gradient between the Veluwe and flanking river plains forces groundwater to be recharged across the Veluwe area and flow toward the lower lying areas. Environmental isotope studies, hydrological analysis, and groundwater flow modeling suggest that the long-term average groundwater recharge across the Veluwe area is $\sim 1 \cdot 10^{-3}$ m/d ($\sim$0.36 m a^{-1}) (i.e., Gehrels, 1999, http://nhi.nu) which is derived from approximately 0.9 m a^{-1} of precipitation. The shallowest sandy units, extending to a depth of 125–200 m, are aquifers in which groundwater flow is relatively unhindered, although the ice-pushed sediments can contain a series of lateral barriers related to glaciotectonic features. Also, in the IJssel valley, clay units occur that limit seepage rates in this area. Regionally, the top of the Miocene clayey formation (Figure 1), which occurs below the sandy aquifers, is regarded as the hydrogeological base below which little groundwater flow occurs (Dufour, 2000).

Between 1978 and 1982, a series of TD profiles were obtained in the Veluwe area using piezometer tubes installed in boreholes. We assume that these TD profiles represent an accurate record of the vertical variation in subsurface temperatures in the geological formations surrounding the boreholes. Likely, the small diameter of the piezometer tube ($50 \cdot 10^{-3}$ m), in combination with the relatively modest vertical thermal gradients below the zone of seasonal influence (i.e., at depths larger than $\sim$15 m), prevents any vertical convection within the piezometers (Colombani et al., 2016). Twenty-nine of the TD profiles in the 1978–1982 data set are deeper than $\sim$100 m, and these are shown in Figure 2a. In the autumn of 2016, several newly constructed boreholes were profiled for temperature in the same area (Figure 2b). During the latter campaign, 10 of the boreholes visited in 1978–1982 were revisited to obtain a direct measurement of subsurface temperature changes at these sites (Figure 3).

The magnitudes of step changes of temperature with depth in the 1978-1982 data indicate that the temperature precision of the thermometer used at the time was on the order of 10^{-2}°C; however, details on calibration controlling absolute accuracy are missing. These historic data were collected at 1 m depth intervals. In 2016, data were collected using a RBR soloT instrument (http://rbr.com) that was calibrated to an accuracy of $2 \cdot 10^{-3}$°C and has a temperature resolution of $<5 \cdot 10^{-6}$°C and a time constant of 1 s. For the 2016 data collection, the stop-go principle (Harris & Chapman, 2007) was used to collect temperature measurements each second for 10 s at each 1 m depth interval.

Piezometer tubes reaching to different known depths are located in the boreholes at each site (Figure 3) which enabled hydraulic head measurements at these depths to be carried out by local authorities on a regular

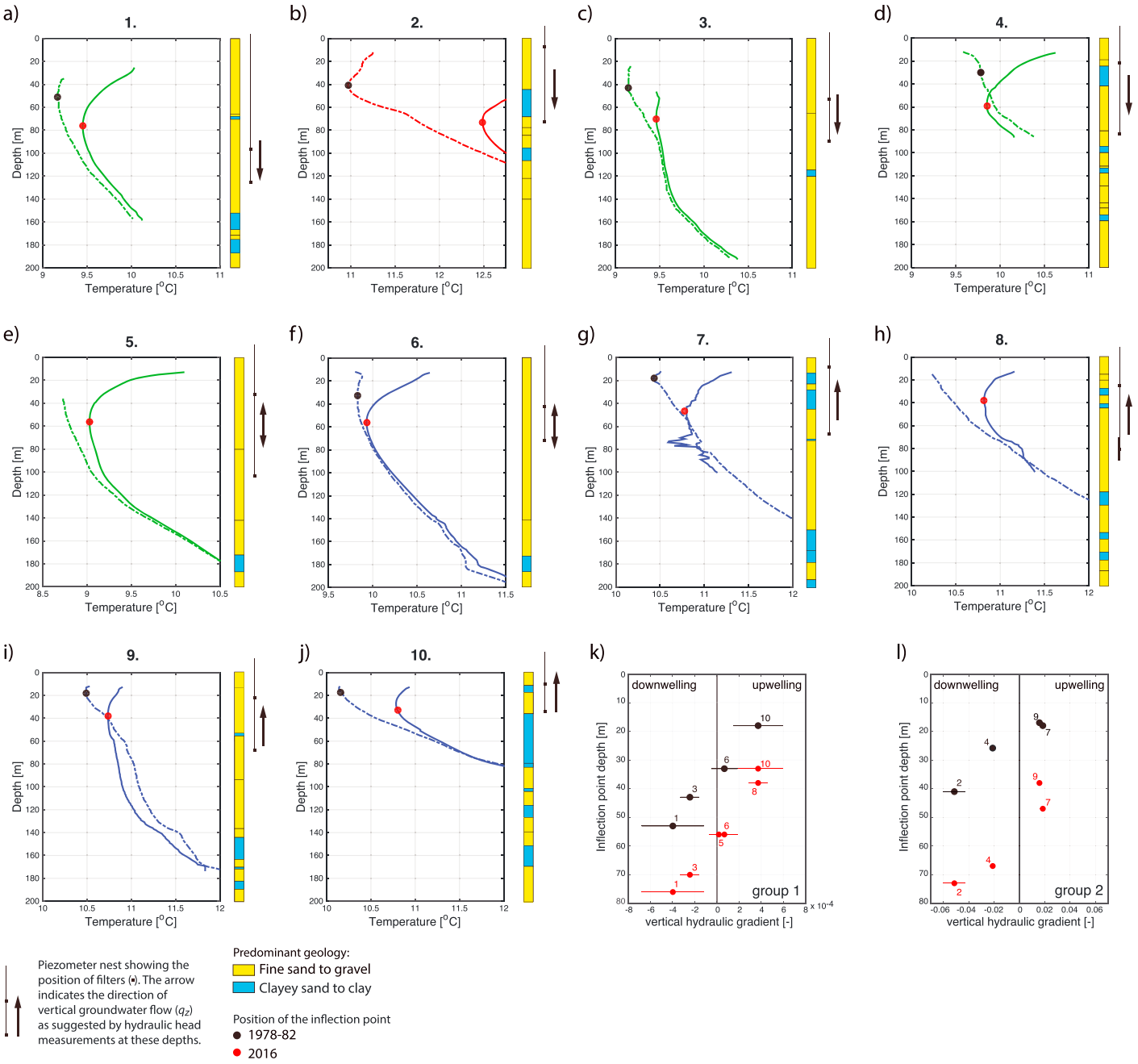

Figure 3. (a to j) Repeated temperature-depth profiles (TD profiles) at sites 1–10 combined with geological information. The dashed lines show the TD profile in the 1978–1982 data set, while the solid lines are TD profiles obtained in 2016. Color of the lines indicates the land use at each site as per Figure 2. Where identifiable, the position of the inflection point is indicated in the diagram (black = 1978–1982 and red = 2016). (k and l) The average annual vertical hydraulic head gradient (1990–2001) at each site is obtained from observations in piezometers and plotted against the depth of the inflection point, also indicating the standard deviation around the mean. Since the downward direction is positive in hydrogeology and flow proceeds in an opposite direction to the hydraulic gradient, a negative (upward) gradient implies positive (downwelling) flow.

basis (e.g., once every 14 days) from the time these boreholes were constructed, mostly in the 1960s and 1970s. However, monitoring was discontinued at many sites in 2000–2001. We accessed a publicly available database (http://dinoloket.nl) containing these hydraulic measurements to evaluate long-term average vertical hydraulic gradients at each of our measurement sites for the years 1990–2001. Additionally, we used a map of average hydraulic head in the shallowest aquifer available for 1995 conditions to evaluate lateral hydraulic head gradients at each borehole site. Also, a detailed description of the lithologies encountered

in each borehole that was recorded at the time of their construction is available. A simplified version of this lithological log is depicted alongside each TD profile in Figure 3.

3. Analysis

3.1. Observed Inflection Point Migration Between 1978 and 2016

For a given depth in each data set of TD profiles (1978–1981 and 2016), there is a substantial range of subsurface temperatures observed (Figure 2). For example, at a depth of 150 m, a range of approximately 4°C is observed in both data sets. At larger depths, this range remains more or less constant, while at shallower depths, it becomes smaller for the 1978–1982 data but increases for the 2016 data. At the base of the seasonal zone, which is estimated to lie at a depth of ~ 15 m for average climatological conditions in the Netherlands (Bense & Kooi, 2004), this contrast in temperature is approximately 2.5°C (1978–1982) and 5.5°C (2016). However, we note that the large range in 2016 temperatures is due to only one urban borehole that is possibly not representative for other urban areas. If this borehole is excluded, the observed temperature range for the 2016 data set is 2.5°C as in 1978–1982.

We identified the potential effects of contrasting land use on the characteristics of the TD profiles by grouping them into three categories (urban areas, forest/shrubs, or grassland/agricultural land) based on their location in the broader region (Figure 1). In both data sets, the relatively cooler TD profiles occur in the forested areas, the warmer ones are in urban areas, and the intermediate profiles lie in grassland/agricultural land (Figure 2). Although the 2016 data set contains more TD profiles taken in forested areas (17 versus 8) and fewer in urban areas (4 versus 8) than the earlier data set, the relationship between the overall temperature of the TD profile with local land use seems consistent between the two data sets. At depths below ~200 m, the TD profiles in both data sets trend toward a thermal gradient of about $2.25 \cdot 10^{-2}$°C m^{-1} with a few exceptions. Since the lithology at these depths for all boreholes consists of the Miocene clay units with presumably similar thermal properties (see Figure 1), the regional background geothermal heat flow is relatively uniform. Assuming a thermal conductivity of 2 W m^{-1}°C^{-1} for these fine marine sediments of Miocene age (Kooi, 2008), the geothermal heat flux at these depths is estimated at $45 \cdot 10^{-3}$ W m^{-2}. This is in agreement with other geothermal heat flux assessments for the Netherlands (e.g., ter Voorde et al., 2014).

Figure 3 presents the temperature-depth data for locations with available measurements in both 1978–1982 and 2016. At depths below which 20th and 21st century climate warming extends (e.g., >120 m), discrepancies in the accuracy and precision between the instruments used in 1978–1982 and 2016 can explain the temperature difference between the two repeated TD profiles up to approximately 0.2°C (sites 1–5 and 10; Figure 3). At site 7, nearby (i.e., ~100–300 m) Aquifer Thermal Energy Storage activities that store or extract heat in geological units cause negative anomalies in the profile below the depth at which the climate warming-related inflection point is visually identified in the profile. At other locations (sites 6, 8 and 9), nearby groundwater abstraction likely has an impact on subsurface temperatures resulting in differences between the historical and current TD profile that cannot be explained from instrumental differences alone. Nevertheless, the thermal inflection point resulting from climate warming was visually identified at all sites in the 2016 data set (Figure 3). For the 1978–1982 data set, the inflection point depth could not be identified for two sites either because there was none visible below a depth of 15 m (site 8) or because the profile was only recorded for the depth interval below which the inflection point was likely located (site 5). Given the precision and accuracy of the thermometers used in 1978–1981 and 2016 and the sampling depth interval of 1 m, we estimate that the inflection point is known to within ±2 m for the 1978–1982 data set and ±0.5 m for the 2016 data.

The inflection point depth in 2016 varies by about 43 m, that is, between 76 m (site 1) and 33 m (site 10). For the 1978–1982 data set a similar range (38 m) exists. The magnitude of the vertical hydraulic head gradient at each site is within one of two groups (1 and 2). For group 1 (Figure 3k), the vertical hydraulic gradients are relatively small ($-8 \cdot 10^{-4}$ to $+6 \cdot 10^{-4}$), while in group 2 (Figure 3l), they are about 2 orders of magnitude larger. In both groups the hydraulic gradient varies between being indicative of either downward (indicated by negative gradient values) or upward (positive gradient values) groundwater flow. The lithological logs (Figure 3) suggest that the larger hydraulic gradients in the second group are probably due to the presence of clayey units that are generally absent in the first group and function as aquitards when present. At sites 5 and 6, hydraulic head gradients suggest that vertical groundwater flow is minimal. On the other hand, sites 1–4 and 7–10 are probably areas of groundwater downwelling and upwelling, respectively. The inflection point depths largely concur with the hydraulic observations in that for decreasing or increasing hydraulic gradients,

the inflection point depth is relatively deep or shallow, respectively. This relationship seems to be approximately linear for both subsets of data (Figures 3j and 3k) and consistent between 1978–1982 and 2016. Further analysis of our data is pursued using a numerical model of subsurface heat flow as outlined below.

3.2. Model Simulation

We used a numerical model to carry out a first-order quantitative analysis of the sensitivity of the inflection point propagation to the magnitude and direction of vertical groundwater flow. We assumed that the development of inflection points in the TD profiles is the result of longer-term ground surface warming, and that the rate at which the inflection point subsequently propagates downward is controlled by subsurface heat flow processes described by the conduction-advection equation for subsurface heat transfer (e.g., Stallman, 1963):

$$\kappa \frac{\partial^2 T}{\partial z^2} - q_z c_w \rho_w \frac{\partial T}{\partial z} = c_b \rho_b \frac{\partial T}{\partial t} \tag{1}$$

in which T (°C) is temperature, z (m) is depth, t is time (s), $c_w\rho_w$ is the volumetric heat capacity of water (J m^{-3}°C^{-1}), κ and $c_b\rho_b$ are the thermal conductivity (W m^{-1} °C^{-1}) and volumetric heat capacity (J m^{-3}°C^{-1}) of the water-saturated aquifer, and q_z (m· s^{-1}) is the vertical component of the specific groundwater flow rate. Here a positive q_z implies groundwater downwelling, while a negative q_z denotes groundwater seepage. In the typical topography-driven groundwater flow system of the Veluwe, we assume that the heat transport mediated by groundwater flow can be accurately described without consideration of thermal dispersion (e.g., see Rau et al., 2012, for a discussion). We used a series of one-dimensional models based upon the numerical solution of equation (1) to facilitate the analysis of the impact of variable hydrogeological conditions (i.e., variations in q_z) on the downward propagation of the inflection point. To this end, we employed the finite-element coding environment FlexPDE (*pdesolutions.com*), which has been previously used to describe transient heat flow in hydrogeological systems (e.g., Bense and Beltrami, 2007). In our modeling approach (cf. Taniguchi et al., 1999), we evaluate the depth-position of the inflection point under different vertical groundwater flow conditions for a set of boundary conditions valid for the study area without aiming to fit the precise shape and temperature of individual TD profiles.

At the base of the model domain, a $45 \cdot 10^{-3}$ W m^{-2} heat flux is imposed, in line with the estimate for the rate of geothermal heat flow derived from the field data as discussed above. We consider a model domain with a fixed height of 150 m, which is the approximate depth to which groundwater flow is generally thought to reach in the study area (Dufour, 2000) (Figure 1). Initially, we assumed that the thermal properties and groundwater flow were uniform within the domain (scenario I). In a second model evaluation (scenario II), we incorporated heterogeneity of thermal properties that would arise from the occurrence of clay units in the stratigraphy as observed in the geological logs (Figure 3). We assume groundwater flow to be purely vertical and invariant with depth. We acknowledge that the vertical components of groundwater flow in a topography-driven flow system (Figure 1c) will decrease with depth both as a result of the geometry of groundwater circulation patterns (Tóth, 1963) as well as reduction of permeability with depth (Rathod & Rushton, 1980). Taking into account multidimensionality of flow to represent a vertically variable groundwater flux and associated heat flow effects would require a more complex multidimensional model which we did not employ in this study. However, a sensitivity study using numerical models was previously conducted (Irvine et al., 2016) and revealed that for steady state conditions, the heat flow effects of lateral groundwater flow are negligible if the horizontal component of groundwater flow does not exceed the vertical flow component by more than 1 order of magnitude. For isotropic hydraulic conductivity, this would result in a ratio between the magnitudes of the vertical (i_z) and horizontal (i_x) head gradients of 0.1. At our sites, this ratio does not fall below 0.2 (Table 1) except where very small vertical head gradients suggest negligible groundwater recharge or discharge (i.e., site 5 and 6). Although Irvine et al. (2016) caution that transient heat flow conditions, such as we consider in the present study, would lower the threshold at which horizontal heat flow can impact groundwater flows inferred from TD profiles, we have carried out our analysis under this assumption. Likewise, we cannot exclude the possibility that the TD profiles in our data set exhibit horizontal conductive effects due to the lateral variability of land use in combination with lateral groundwater flow as described by Bense and Beltrami (2007). An evaluation of our data for such effects would require an inventory of historical land use around each borehole site in combination with an analysis of local groundwater flow paths, which has not been undertaken in this study.

Carrying forward with the assumptions and model setup as described above, we set a constant ground surface temperature to calculate steady state TD profiles for a range of plausible q_z values (−0.1–0.6 m a^{-1}),

Table 1
Inflection Point Depths (IFD), Hydraulic Gradients (i), and Inferred Vertical Groundwater Fluxes (q_z) at Sites 1–10

	IFD (m)		i (10^{-4} m m^{-1})			q_z (m a^{-1})	
Site	1978–1982	2016	$\bar{i}_z \pm \sigma$	i_x	$\lvert i_z{:}i_x \rvert$	I	II
1.	53	76	−3.95 ± 2.81	19.5	0.20	0.20	0.24
2.	41	73	−515 ± 88.2	4.6	110.88	0.16	0.19
3.	43	70	−2.45 ± 0.85	11.1	0.22	0.16	0.19
4.	27	67	−211 ± 18.1	20.4	10.34	0.11	0.14
5.	–	56	0.18 ± 0.89	7.8	0.02	0.09	0.11
6.	33	56	0.67 ± 1.18	29.6	0.02	0.07	0.10
7.	18	47	184 ± 18	7.8	23.51	0.02	0.05
8.	–	38	3.72 ± 0.87	7.0	0.53	−0.02	0.02
9.	17	38	158 ± 2	29.9	5.29	0.00	0.03
10.	18	33	3.73 ± 2.23	9.8	0.38	−0.02	−0.01

Note. Vertical hydraulic head gradients (i_z) at each site are obtained from piezometer readings (see Figure 3) and reported as averages of the annual mean between 1990 and 2001 with the standard deviation from the mean value. Horizontal hydraulic gradients (i_x) in the upper aquifer at each site are representative for the annual average situation in 1995. Estimates of q_z (m a^{-1}) at each site are derived by finding the best fit between field observations at each site of the inflection point depth in 1978-82 and 2016 with a single theoretical curve. This was done for the two model scenarios (I and II) as shown in Figure 4.

standard values for $c_w\rho_w$, and for a homogeneous domain (scenario I) representing a fully sandy aquifer as well as a domain with heterogeneity in the thermal properties (scenario II) that incorporates clay units of lower thermal diffusivity. Parameter values of thermal properties are based upon values reported by Kooi (2008) for the sediments in the study area. These values are $\kappa = 2.0$ W m^{-1}°C^{-1}, $c_b\rho_b = 2.5\ 10^6$ J m^{-3}°C^{-1} for sand and $\kappa = 1.2$ W m^{-1}°C^{-1}, $c_b\rho_b = 2.8 \cdot 10^6$ J m^{-3}°C^{-1} for clay. In our approach to simulate the depth migration of the inflection point, we do not need to specifically evaluate the offset between surface air temperature and ground surface temperature as is required in other approaches (e.g., Bense et al., 2017). We do assume, however, that the long-term rate of increase in surface air temperature as recorded by meteorological stations in the area (Figure 4a) is congruent with the long-term rise in ground surface temperature. Using each steady state model as the initial conditions, we induced transience by increasing the ground surface temperature at a rate based on the long-term average trend indicated by the recorded surface air temperature data (Figure 4a). We acknowledge that in areas of urban development, or other types of land use change, this regional trend might underestimate the true surface warming. Since the transient model runs were initiated in 1906 and completed in 2016, we do not consider the effect of any subsurface thermal disturbance that might have been present resulting from climate warming prior to 1906.

The model results were used to generate a set of curves showing the theoretical progression of the inflection point in time for a range of groundwater fluxes, one specific ground surface temperature trend (Figure 4a), and for homogeneous (scenario I; Figure 4b) and heterogeneous thermal properties (scenario II; Figure 4c). These time continuous model curves are shown alongside the observations of inflection point depth in 1978–1982 and 2016.

4. Discussion and Conclusions

The modeling results (Figures 4b and 4c) illustrate how climate warming and groundwater flow conditions control both the initial development of an inflection point, as well as its downward propagation into the subsurface. When no vertical groundwater flow is considered ($q_z = 0$), the rate of surface warming prior to the mid-1960s ($0.6 \cdot 10^{-2}$°C a^{-1}; Figure 4a) is not sufficient to generate an inflection point. However, in areas of groundwater downwelling, an inflection point develops quickly after the onset of warming in 1906 and starts to propagate downward at a rate strongly coupled to the rate of vertical groundwater flow. Inflection points develop in areas of little or no downward groundwater flow, but only after surface warming rates accelerate to a level of $\sim 3.1 \cdot 10^{-2}$°C a^{-1} from the late 1970s onward. In areas where groundwater upwelling exceeds −0.1 m a^{-1}, results from both model domains (I and II) suggest that by 2016, no inflection point would have

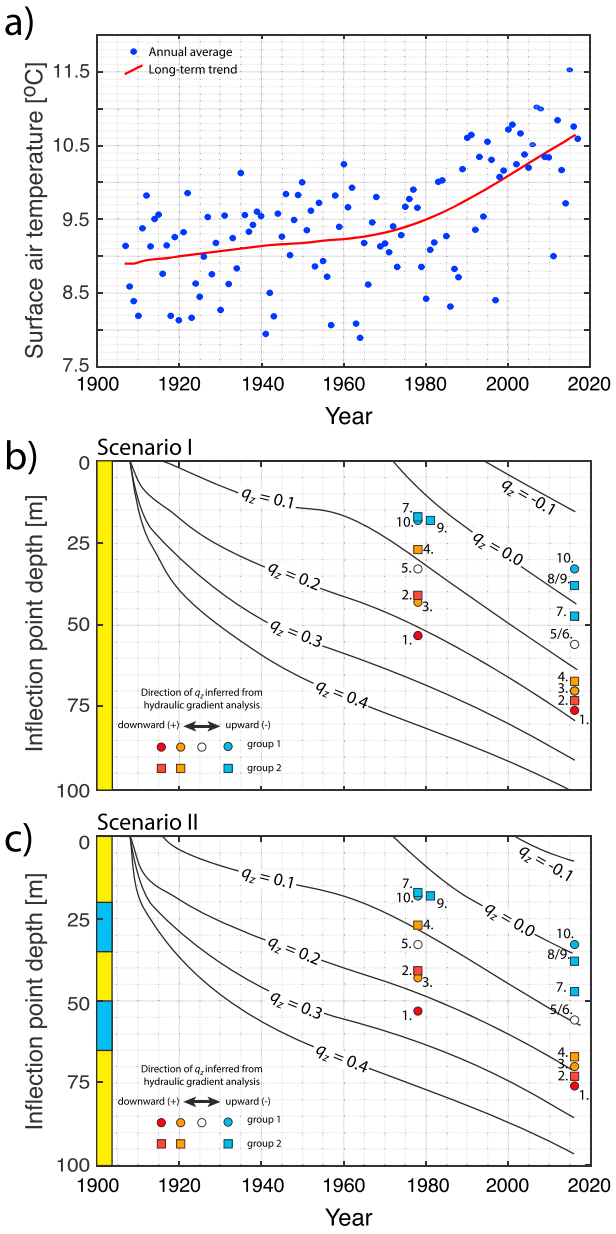

Figure 4. Model results and comparison to observed data. (a) Subsurface warming is forced by increasing the ground surface temperature (the upper boundary of the model) in accordance with the long-term trend (red line) inferred from annual average surface air temperatures representative for the central part of the Netherlands including the Veluwe area (van der Schrier et al., 2011; Visser & Petersen, 2012). Model simulations of the sensitivity to vertical groundwater flow of the inflection point depth in the TD profile in time for (b) homogeneous thermal properties (scenario I) in an aquifer composed of sandy material (yellow), and (c) when thermal properties are heterogeneous as a result of the presence of clayey (blue) units in an otherwise sand-dominated aquifer (scenario II). In Figures 4b and 4c, observed inflection point depths (see Figure 3) are indicated by symbols labeled with numbers corresponding to each sites 1–10. The infill color of the symbols highlights the relative magnitude of the observed hydraulic head gradient and the inferred direction of the vertical groundwater flux, while the shape of the symbol denotes in which hydraulic head gradient group (1 or 2; see Figures 3k and 3l) each site falls.

penetrated to a depth exceeding that of the seasonal zone (at a depth of ~15 m), which would make it practically difficult to detect unless TD profiles in the seasonal zone are repeated through one seasonal cycle (e.g., Bense & Kooi, 2004). The inclusion of clay units with a reduced thermal conductivity compared to an otherwise sandy subsurface (model scenario II) does somewhat retard the propagation of the inflection point in the model, but not in a significant way as indicated by a comparison of Figure 4b and Figure 4c.

The increase of the inflection point depth as observed for the sites (1–10) in our data set is in agreement with the range of modeled inflection point propagation rates for different values of q_z (Figures 4b and 4c). The model results suggests that q_z varies between small rates of groundwater upwelling (sites 9 and 10) and groundwater downwelling for all other sites (1–8), up to a maximum of ~0.2–0.24 m a^{-1} for site 1 (Table 1). This is a plausible range of groundwater downwelling rates across the Veluwe that is in agreement with groundwater recharge estimates for the general Veluwe area from isotope studies and groundwater model evaluations (i.e., Gehrels, 1999, http://nhi.nu). These former studies indicate that recharge rates rarely exceed ~0.35 m a^{-1} and are probably lower at many locations. Since a uniform vertical groundwater flux is assumed in our 1-D model as a simplification of a system in which the vertical groundwater flow component probably decreases with depth, our inferred groundwater fluxes should be interpreted as a depth-averaged value and hence are an underestimate of the groundwater recharge flux across the near-surface water table. Additionally, we compared the independent assessment of the groundwater fluxes at each site based upon our thermal modeling exercise with the evaluation of vertical groundwater flow conditions based upon the analysis of vertical hydraulic head gradients (Figures 3j and 3k). This yields some discrepancies. For example, at sites 7–9, hydraulic gradients suggest upward fluxes (Figures 3k and 3l), while the model-derived q_z values (Figure 4b) for 1978 suggest either no flow or a downward flux that is equal to (site 7) or smaller than 0.1 m a^{-1}. However, by 2016, a comparison of the measured inflection point depths and the model results (Figure 4b) indicates that sites 8-10 are in an upwelling zone, in agreement with the hydraulic gradient data (Figures 3k and 3l). Such discrepancies are possibly resolved if in future studies the multidimensionality of groundwater flow and its impact on the subsurface heat flow regime is considered in conjunction with, local deviations from the regional trend in surface temperature warming resulting from land use change, water table fluctuations, or other near-surface environmental variables. Regardless, since no direct measurements of vertical groundwater flow rates are otherwise available for any of these sites, it is not possible to truly validate the flow rates inferred from the inflection point migration analysis. We note that the same is true for virtually all methods that are independently used to estimate relatively deep vertical groundwater fluxes (Ferguson & Woodbury, 2005; Irvine et al., 2017; Scanlon et al., 2006).

TD data in our study area clearly reflect land use conditions as subsurface temperatures in forested areas are several °C lower than in flanking grassland and urban areas (Figure 2). However, additional controls on subsurface temperature by vertical groundwater flow have long been known to hamper the full potential of TD profile data to quantify interactions between surface environmental change and consequent changes in subsurface temperature patterns. We demonstrate here that vertical groundwater flow rates, in particular groundwater downwelling, can be inferred

independently from these other thermal disturbances solely by tracking the depth propagation of TD profile inflection points resulting from sustained ground surface warming. Our results suggest that tracking thermal inflection points through TD profiling has the potential to be a powerful groundwater tracer technique that opportunistically exploits the effects of climate warming on subsurface thermal regimes.

Acknowledgments
TNO Build Environment is acknowledged for archiving and providing the 1978–1982 data set. The water company Vitens is thanked for allowing access to wells belonging to their groundwater observation network. Christian de Kleijn is thanked for help with field data collection. Bayani Cardenas, Philipp Blum, Grant Ferguson, and an anonymous reviewer commented constructively on an earlier version of the manuscript which led to a significant improvement of the quality of this letter. All data used in this letter are available through dinoloket.nl that which is the main portal to hydrogeological data in the Netherlands.

References

Bayer, P., Rivera, J. A., Schweizer, D., Schärli, U., Blum, P., & Rybach, L. (2016). Extracting past atmospheric warming and urban heating effects from borehole temperature profiles. *Geothermics*, *64*, 289–299. https://doi.org/10.1016/j.geothermics.2016.06.011

Bense, V., & Beltrami, H. (2007). Impact of horizontal groundwater flow and localized deforestation on the development of shallow temperature anomalies. *Journal of Geophysical Research*, *112*, F04015. https://doi.org/10.1029/2006JF000703

Bense, V. F., & Kooi, H. (2004). Temporal and spatial variations of shallow subsurface temperature as a record of lateral variations in groundwater flow. *Journal of Geophysical Research*, *109*, B04103. https://doi.org/10.1029/2003JB002782

Bense, V. F., Kurylyk, B. L., van der Ploeg, M. J., van Daal, J., & Carey, S. (2017). Interpreting repeated temperature-depth profiles for groundwater flow. *Water Resources Research*, *53*, 8639–8647. https://doi.org/10.1002/2017WR021496

Bredehoeft, J. D., & Papadopulos, I. S. (1965). Rates of vertical groundwater movement estimated from the Earth's thermal profile. *Water Resources Research*, *1*(2), 325–328.

Colombani, N., Giambastiani, B. M. S., & Mastrocicco, M. (2016). Use of shallow groundwater temperature profiles to infer climate and land use change: Interpretation and measurement challenges. *Hydrological Processes*, *30*, 2512–2524. https://doi.org/10.1002/hyp.10805

Davis, M. G., Harris, R. N., & Chapman, D. S. (2010). Repeat temperature measurements in boreholes from northwestern Utah link ground and air temperature changes at the decadal time scale. *Journal of Geophysical Research*, *115*, B05203. https://doi.org/10.1029/2009JB006875

Dědeček, P., Šafanda, J., & Rajver, D. (2012). Detection and quantification of local anthropogenic and regional climatic transient signals in temperature logs from Czechia and Slovenia. *Climatic Change*, *113*(3), 787–801.

Dufour, F. (2000). Groundwater in the Netherlands: Facts and figures. Netherlands Institute of Applied Geoscience TNO, Delft.

Ferguson, G., Beltrami, H., & Woodbury, A. D. (2006). Perturbation of ground surface temperature reconstructions by groundwater flow? *Geophysical Research Letters*, *33*, L13708. https://doi.org/10.1029/2006GL026634

Ferguson, G., & Woodbury, A. (2005). The effects of climatic variability on estimates of recharge from temperature profiles. *Ground Water*, *43*, 837–842.

Ferguson, G., & Woodbury, A. D. (2007). Urban heat island in the subsurface. *Geophysical Research Letters*, *34*, L23713. https://doi.org/10.1029/2007GL032324

Gehrels, J. C. (1999). Groundwater level fluctuations: Separation of natural from anthropogenic influences and determination of groundwater recharge in the Veluwe area, the Netherlands. Vrije Universiteit.

Harris, R. N., & Chapman, D. S. (2007). StopâĂŘ-go temperature logging for precision applications. *Geophysics*, *72*(4), E119–E123. https://doi.org/10.1190/1.2734382

Irvine, D. J., Cartwright, I., Post, V. E., Simmons, C. T., & Banks, E. W. (2016). Uncertainties in vertical groundwater fluxes from 1-D steady state heat transport analyses caused by heterogeneity, multidimensional flow, and climate change. *Water Resources Research*, *52*(2), 813–826. https://doi.org/10.1002/2015WR017702

Irvine, D. J., Kurylyk, B. L., Cartwright, I., Bonham, M., Post, V. E., Banks, E. W., & Simmons, C. T. (2017). Groundwater flow estimation using temperature-depth profiles in a complex environment and a changing climate. *Science of The Total Environment*, *574*, 272–281. https://doi.org/10.1016/j.scitotenv.2016.08.212

Kooi, H. (2008). Spatial variability in subsurface warming over the last three decades; insight from repeated borehole temperature measurements in the Netherlands. *Earth and Planetary Science Letters*, *270*(1), 86–94.

Kurylyk, B., Irvine, D., Carey, S., Briggs, M., Werkema, D., & Bonham, M. (2017). Heat as a groundwater tracer in shallow and deep heterogeneous media: Analytical solution, spreadsheet tool, and field applications. *Hydrological Processes*, *31*(14), 2648–2661.

Kurylyk, B. L., & Irvine, D. J. (2016). Analytical solution and computer program (FAST) to estimate fluid fluxes from subsurface temperature profiles. *Water Resources Research*, *52*, 725–733.

MacDougall, A. H., & Beltrami, H. (2017). Impact of deforestation on subsurface temperature profiles: Implications for the borehole paleoclimate record. *Environmental Research Letters*, *12*(7), 074,014.

Menberg, K., Blum, P., Kurylyk, B. L., & Bayer, P. (2014). Observed groundwater temperature response to recent climate change. *Hydrology and Earth System Sciences*, *18*, 4453–4466. https://doi.org/10.5194/hess-18-4453-2014

Rathod, K. S., & Rushton, K. R. (1980). Flow in aquifers when the permeability varies with depth. *Hydrological Sciences Bulletin*, *25*(4), 395–406. https://doi.org/10.1080/02626668009491949

Rau, G. C., Andersen, M. S., & Acworth, R. I. (2012). Experimental investigation of the thermal dispersivity term and its significance in the heat transport equation for flow in sediments. *Water Resources Research*, *48*, W03511. https://doi.org/10.1029/2011WR011038

Reiter, M. (2001). Using precision temperature logs to estimate horizontal and vertical groundwater flow components. *Water Resources Research*, *37*, 663–674.

Saar, M. O. (2011). Review: Geothermal heat as a tracer of large-scale groundwater flow and as a means to determine permeability fields. *Hydrogeology Journal*, *19*(1), 31–52.

Scanlon, B. R., Keese, K. E., Flint, A. L., Flint, L. E., Gaye, C. B., Edmunds, W., & Simmers, I. (2006). Global synthesis of groundwater recharge in semiarid and arid regions. *Hydrological Processes*, *20*, 3335–3370.

Stallman, R. W. (1963). Computation of ground-water velocity from temperature data. vol. 1544-H, water supply paper Methods of Collecting and Interpreting Ground-Water Data, USGS, Washington, DC, USA.

Taniguchi, M., Shimada, J., Tanaka, T., Kayane, I., Sakura, Y., Shimano, Y., … Kawashima (1999). Disturbances of temperature-depth profiles due to surface climate change and subsurface water flow: 1. An effect of linear increase in surface temperature caused by global warming and urbanization in the Tokyo metropolitan area, Japan. *Water Resources Research*, *35*(5), 1507–1517.

ter Voorde, M., van Balen, R., Luijendijk, E., & Kooi, H. (2014). Weichselian and Holocene climate history reflected in temperatures in the upper crust of the Netherlands. *Netherlands Journal of Geosciences/Geologie en Mijnbouw*, *93*(3), 107–117. https://doi.org/10.1017/njg.2014.9

Tóth, J. (1963). A theoretical analysis of groundwater flow in small drainage basins. *Journal of Geophysical Research*, *68*, 4795–4812.

van der Schrier, G., van Ulden, A., & van Oldenborgh, G. J. (2011). The construction of a Central Netherlands temperature. *Climate of the Past*, *7*, 527–542. https://doi.org/10.5194/cp-7-527-2011

Visser, H., & Petersen, A. C. (2012). Inferences on weather extremes and weather-related disasters: A review of statistical methods. *Climate of the Past*, *8*, 265–286. https://doi.org/10.5194/cp-8-265-2012

Wada, Y., van Beek, L. P. H., van Kempen, C. M., Reckman, J. W. T. M., Vasak, S., & Bierkens, M. F. P. (2010). Global depletion of groundwater resources. *Geophysical Research Letters*, *37*, L20402. https://doi.org/10.1029/2010GL044571